BIOMECHANICS OF BUTTRESSED TREES: BENDING STRAINS AND STRESSES[1]

BRUNO CLAIR,[2] MERIEM FOURNIER,[2,5] MARIE FRANÇOISE PREVOST,[3]
JACQUES BEAUCHENE,[2] AND SANDRINE BARDET[4]

[2]UMR, Ecologie des Forêts de Guyane, CIRAD ENGREF INRA, Campus Agronomique, BP 709, 97310 Kourou, Guyane Française,
France; [3]UMR, Botanique et Bioinformatique de l'architecture des plantes AMAP, IRD Centre de Cayenne, BP 165, 97323
Cayenne, Guyane Française, France; and [4]Laboratoire de Mécanique et de Génie Civil, UMR 5508 CNRS Université de Montpellier
II, cc 081, Bat 13, Place Eugene Bataillon, 34095 Montpellier Cedex 5, France

The different hypotheses about buttress function and formation mainly involve mechanical theory. Forces were applied to two trees of *Sloanea* spp., a tropical genus that develops typical thin buttresses, and the three-dimensional strains were measured at different parts of the trunk base. Risks of failure were greater on the buttress sides, where shear and tangential stresses are greater, not on the ridges, in spite of high longitudinal (parallel to the grain) stresses. A simple beam model, computed from the second moment of area of digitized cross sections, is consistent with longitudinal strain variations but cannot predict accurately variations with height. Patterns of longitudinal strain variation along ridges are very different in the two individuals, owing to a pronounced lateral curvature in one specimen. The constant stress hypothesis is discussed based on these results. Without chronological data during the development of the tree, it cannot be proved that buttress formation is activated by stress or strain.

Key words: biomechanics; buttress; Eleaocarpaceae; French Guiana; *Sloanea* spp.; tropical trees; wood.

Buttresses, lateral flanges joining the roots and the trunk, have intrigued generations of biologists. Large buttresses are quite rare in temperate areas, but very characteristic among a remarkable variety of tropical stem forms. Buttress occurrence and form within one species are quite fixed traits, although some species are relatively variable in this respect. Buttress characterization is also of significant practical interest in identifying tropical trees (Gentry, 1993). A number of different biological theories have tried to explain the function and the formation of buttresses (Kaufman, 1988; Richards, 1995). Some authors assumed that physiological stresses force aerial development of shallow root systems (Halle et al., 1978). Others assumed that buttresses prevent climbing by woody vines or reduce competition with other trees by occupying available space (Black and Harper, 1979). Lastly, as the term "buttress" suggests, there is a general consensus that these structures are of mechanical importance (Kaufman, 1988; Mattheck, 1991; Ennos, 1993, 1995; Young and Perkocha, 1994; Chapman et al., 1998). However the actual function has not been empirically demonstrated, and such theories assume that buttresses are of adaptive value in resisting wind or gravity forces or are formed via mechanistic constraints based on hypotheses of stimulated growth in mechanically stressed zones of the trunk base.

There is only limited experimental and theoretical work on how buttresses act mechanically. Mattheck's group (Mattheck, 1990, 1991; Mattheck and Prinz, 1991) assumed that cambial growth is activated by stress and simulated stresses induced by a bending moment at the stem base via a finite element model. By an incremental process that was supposed to simulate peripheral secondary growth in the tree (Mattheck, 1990), material was added step by step at the wood surface, where mechanical stresses are greater. Mechanical stresses were analyzed at each step, until they became constant all around the trunk and buttress surfaces, under different testing boundary conditions that simulated anchorage between buttresses and underground soil or roots. The forms predicted by Mattheck's model were finally compared to existing ones in nature. Mattheck's model can explain many patterns of buttress form and development observed by ecologists (Ennos, 1993). Although some of the assumptions from such approaches are questionable, such types of mechanical hypotheses need to be validated by experimental measurements of geometries, material properties, and strains.

Ennos (1995) and Crook et al. (1997) discussed Mattheck's theory with simulated windthrow tests and morphological observations of roots after working on Malaysian trees with and without buttresses. They observed root movements and trunk displacement, strains along buttresses, trunk and anchorage strength, and crack modes on both the leeward and windward sides.

In this paper, we present experimental results based on a typical buttressed genus in the lowland tropical rainforest of French Guiana. The aim was to localize the risks of failure by directly measuring strains and to discuss Mattheck's constant stress hypothesis in the light of these results. We also tested the ability of a simple beam model to describe strain patterns under external bending forces.

MATERIALS AND METHODS

Materials—After looking at typical buttresses on small diameter trees, we selected the genus *Sloanea* (Eleaocarpaceae), because ". . . a good habit character is the usual development of unusually thin, frequently large buttresses . . . " (Gentry, 1993, p. 395). This genus is represented by 17 species in French Guiana (Hollowel et al., 2001), 60–70 species in tropical America, and 120 species in the world, all of which are tropical in distribution (Gentry,

1993; Mabberley, 1997). The two trees used in the this experiment were of the same size (20 cm DBH) and located in rainforest in the "Piste St. Elie" field station (53°0′ W–5°20′ N). Both trees had three well-developed and thin buttresses. However, in the first tree, buttresses are straight, approximately triangular "plates." In the second one, the buttress flanges have lateral curvatures. Specimens have been donated to the international herbarium of Cayenne. The first tree has been identified as *Sloanea* cf. *tuerckheimii* J. D. Smith; the second one is a different species that has not yet been identified.

Field experiments—Local strains were measured at the periphery of standing trees. The strain sensors were attached on peripheral wood, after removing the thin bark, in order to measure wood behavior because wood is the main support tissue. In buttresses, strains were measured with strain gauge sensors (DD1 type; Hottinger Baldwin Messtechnik, Darmstadt, Germany) connected in full bridge mode to a battery-powered strain bridge (Alco system, Captels, S. Matthieu de Treviers, France). The sensors were fitted with steel pins, spaced 13 mm apart. The accuracy of this system of measurement is estimated at 30 microstrains (i.e., 30 μm/m).

The bending experiment is illustrated in Fig. 1. The trunk was pulled with a manual winch, using a steel cable anchored to the base of another tree nearby. The applied force was measured with a field load cell (Captels). Forces were applied at a height of 5 m in five stages. The main aim during testing was to remain within the intact structural and linearly elastic material properties; strains were measured at different locations along the ridges and on the sides of the three buttresses by moving the sensors between successive experiments. This approach assumed and checked that the behavior was linear and elastic, so that experiments were repeatable. A mechanical extensometer (Fournier et al., 1994) was fixed on the trunk just above the buttresses and was not moved between successive tests. This ensured repeatability while defining the maximal applied loads. A strain control was chosen with a maximum of -1000 microstrains in the compressed wood of the trunk above the buttresses. After checking the linearity of each test, the slopes ε_L/F, ε_T/F, ε_{45}/F (ε_L represents strain along the grain or longitudinal [L] strain, ε_T represents strain perpendicular to the grain or tangential [T] strain, ε_{45} represents strain parallel to the diagonal between L and T direction, and F represents applied force) were computed from all five levels of applied force and analyzed for each measurement. According to the definition of the strain tensor and mathematical formulas for axes changes (Berthelot, 1999), the shear strain ε_{LT}/F was calculated as

$$\varepsilon_{LT}/F = \varepsilon_{45}/F - (\varepsilon_L/F + \varepsilon_T/F)/2.$$

Two sets of bending tests were performed by reversing the direction of force: in both sets, buttress A was lined up with the direction of force. In the first set, this buttress was put into tension; in the second set, the buttress was put into compression.

On the second tree, the force direction was also parallel to one buttress, put in compression. We measured longitudinal strains along the ridge of this buttress and shear strains at two opposite points of the lateral sides. In a final test, we increased the load until the buttress broke and observed how and where the break was initiated.

Model of bending strains—A simple model for longitudinal bending strains has been designed at the cross section level based on beam theory (strength of materials) that is often used to compute stresses and strains in slender plant axes (Niklas, 1992). The model (see Appendix) uses the following data: the two components (vertical parallel to the trunk and horizontal) of the applied force, the lever arm (vertical distance from the cross section to the applied force), the geometrical characteristics of the cross section (the cross sectional area and the second moments of area that are the relevant geometrical variables to predict flexural stiffness at the cross section level [Niklas, 1992]), and wood stiffness (i.e., Young's modulus of elasticity of green wood as measured parallel to the grain).

As the model predicts that the longitudinal strain ε_L is proportional to the applied force F and to the modulus of elasticity E_L, we will compare theoretical and experimental results by analyzing linear regressions between experimental slopes ε_L/F and theoretical values of ε_L/E_LF. The slopes of these regressions are estimations of the modulus of elasticity E_L.

Additional data—At the end of the field experiment, the tree was felled above the buttresses. To characterize cross section geometries, slices 10 cm thick with parallel and horizontal surfaces were carefully sawn from the buttresses. In the laboratory, each surface was photographed and analyzed with the software Optimas 6.5 (Media Cybernetics, Silver Spring, Maryland, USA) to define the outlines and compute (standard functions) for each height x, the center of mass position, the area $S(x)$, and the second moments of area I_y, $I_z(x)$ and $I_{yz}(x)$.

Wood basic density (ratio of oven-dried mass to saturated volume) was measured within buttress A (seven heights, three radial positions for each height, two samples for each position), as dried wood density is a good predictor of elastic properties (Kollman and Cote, 1968; Guitard, 1987; Niklas, 1992). Moreover, we adjusted the measured values of basic density to estimate air-dried (i.e., wood moisture content of 12%) density: drying shrinkage is supposed to account for 0.6% of volume per percentage of moisture content loss (CIRAD Forêt database on tropical woods, properties of *Sloanea* spp., J. Gérard, CIRAD Forêt, Montpellier, France, personal communication) and therefore air-dried density is 1.25 times basic density. We then calculated the modulus of elasticity E_{Lad} of air-dried wood, from Guitard's regressions (Guitard, 1987). The green wood assessment 0.73 E_{Lad} (Kollman and Cote, 1968) were compared to the mentioned slopes of regression. Lastly, Young's moduli have been measured by tensile tests on air-dried wood samples by the method still used by Clair et al. (2003) and compared to other estimations.

RESULTS

Linearity, elasticity, and repeatability—As expected, each strain measurement had a linear response to the applied force: $r^2 > 0.9$ in 83% of the 355 analyzed force vs. strain curves, $r^2 < 0.6$ in only 3% of analyzed curves. The strain returned to zero after unloading. Repeatability was very good and, for each test, the slope of the force-strain curve could be calculated. Within each set of tests, the variations of these slopes was very small (CV < 6%), with no systematic change with time.

Strain and force magnitudes—During all the bending experiments, measured strains in the different parts of buttresses remained between -3000 microstrains and 2000 microstrains along the grain, -5000 microstrains and 1200 microstrains in the tangential direction, below green wood elastic limit, but often much higher than the controlled maximal strain in the trunk of -1000 microstrains. The maximum bending moments about the base of the tree were 23 500 Nm in the first set and 20 000 Nm in the second. Maximal forces were about 5000 N.

As expected, longitudinal strains, which are the most intuitively predictable, were positive (stretching) on buttresses under tension, compressive (shrinking) in the opposite ones. When the force direction was reversed (second set of tests), strains were obviously of opposite sign, but of the same magnitude, along the ridges (Fig. 2) and on the buttress sides.

Mean absolute values of longitudinal and shear strains per unit of basal bending moment, $\varepsilon_L/FL \cos \theta$ and $\varepsilon_{LT}/FL \cos \theta$, had the same scale of magnitude, 0.022 microstrains/Nm and 0.017 microstrains/Nm, respectively. Tangential strains were slightly lower (mean value 0.013 microstrains/Nm). Longitudinal and tangential strains were opposite and had a significant negative correlation ($r^2 = 0.30$), with a slope of -0.64 (Fig. 3). When the data were split, the correlation was greater ($r^2 = 0.53$) when keeping only the points closest to the ridge (<10 cm), but it was not significant when these points were removed. Although an exhaustive study of shear strains was not performed in every part of the three buttresses, smaller values for all strain components have been measured in but-
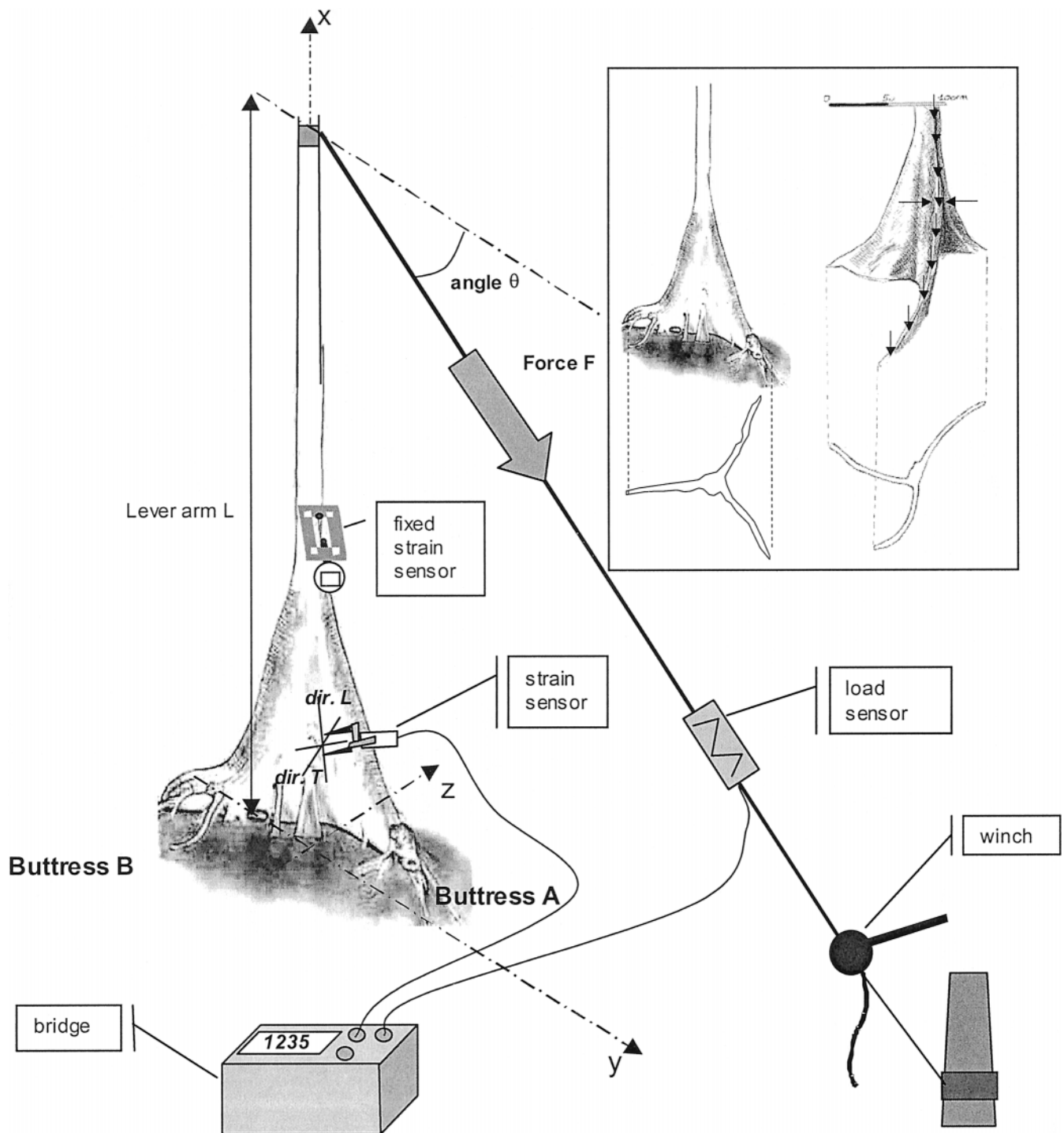
Fig. 1. Design of the bending tests and buttress forms of trees of *Sloanea* spp. Inset: left, first tree, with flat buttresses; right, second tree, with curved buttresses. On the first tree, measurements were made in every part of the buttressed zone. On the second tree, the locations of the measurements are indicated by arrows.

tresses B and C not parallel to the applied force. Therefore, the following discussion is mainly focused on observations of buttress A.

Spatial variations of strains—On the first tree, longitudinal strains were nearly constant along the ridges, excepted in the first measured points near the ground at the tip of the root

where they were very small (Fig. 2). They decreased on the sides, from the buttress ridge to the central trunk (Fig. 4).

On the opposite side, shear strains were minimal near the ridges and reached maximal values on sides near the trunk (Fig. 5). In the main buttress studied, buttress A, strain patterns were similar between the two sides. In the two lateral buttresses, some discrepancies were observed from one side to the
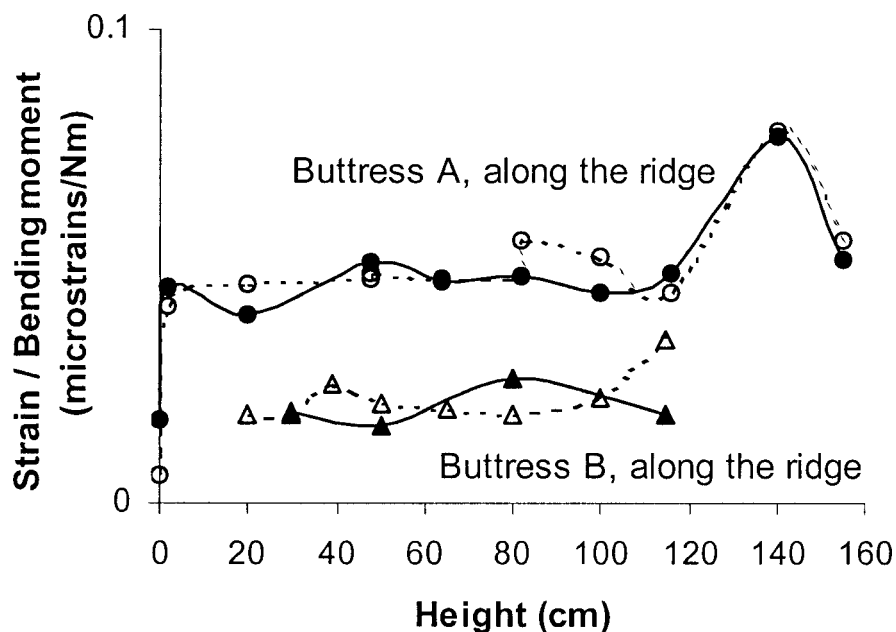
Fig. 2   Longitudinal strains measured along the buttress ridges during bending tests performed on one tree of *Sloanea* cf. *tuerckeimii*. Solid lines, buttress A is in tension; dotted lines, buttress A is in compression. Circles, results related to buttress A; triangles, results related to buttress B. To allow comparisons, the ratio of strains to the basal bending moment is represented, with absolute values of strains.

other, but no systematic variations were found, and actually, values of strains were often small.

On the second tree, longitudinal strains on the buttress ridge in parallel to the applied force increased continuously from the base to the top (Fig. 6). We did only one measurement of the three-dimensional strain, near the trunk, at 50 cm height, on both buttress sides (Fig. 1). In fact, shear strain was high (0.05 microstrains/Nm) on the concave side, but almost zero (0.003 microstrains/Nm) on the convex opposite one. The ratio $\varepsilon_T/\varepsilon_L$ was -1.5 on the concave side, 1 on the opposite one.

Observations about breakage—Breakage was initiated by cracking the wood at the buttress plate (Fig. 7). The longitudinal crack began inside the concave side of the buttress put in compression. No uprooting was observed.
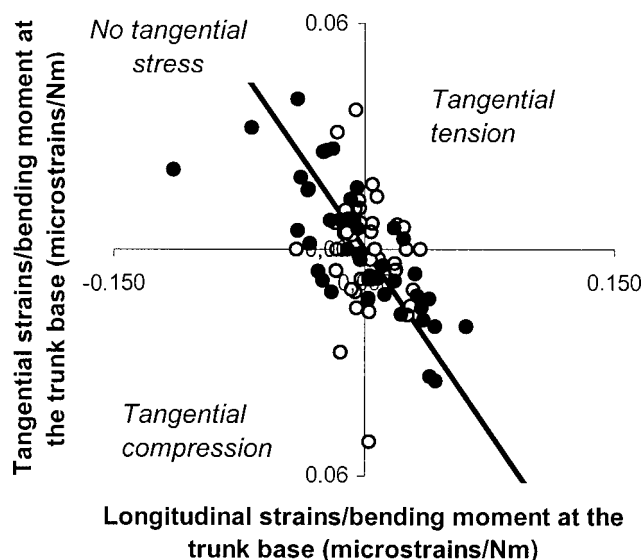

Fig. 3.   Tangential strains vs. longitudinal strains measured during bending tests performed on one tree of *Sloanea* cf. *tuerckeimii*. Open circles represent the zones closest to the ridge (<10 cm). Filled circles represent the sides. The regression is calculated for all the points and is significant ($r = -0.55$, $P < 0.001$). The regression line is the principal axis, because both variables play a symmetrical role.
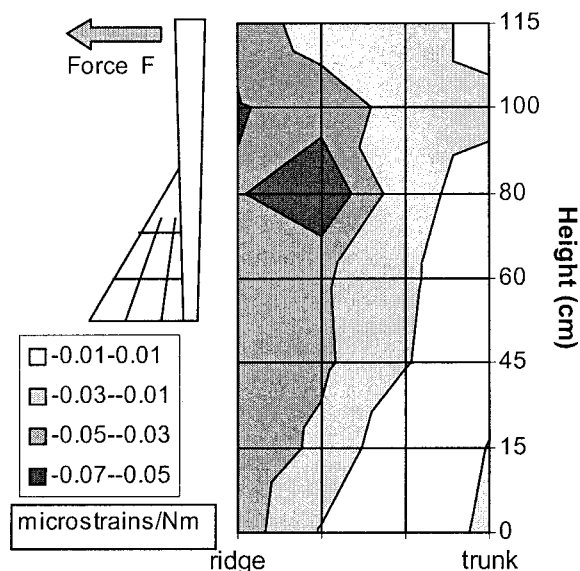

Fig. 4.   Measured longitudinal strains per unit of bending moment at the trunk base of *Sloanea* cf. *tuerckeimii*, on buttress A side. The buttress and the force are in the same plane, and the buttress is in compression (negative values). Results are given for one side of the buttress as a function of height and distance to the ridge.

Fig. 5.   Measured shear strains per unit of bending moment at the trunk base of *Sloanea* cf. *tuerckeimii*, on buttress A side. The buttress and the force are in the same plane, and the buttress is in compression (negative values). Results are given for one side of the buttress as a function of height and distance to the ridge.
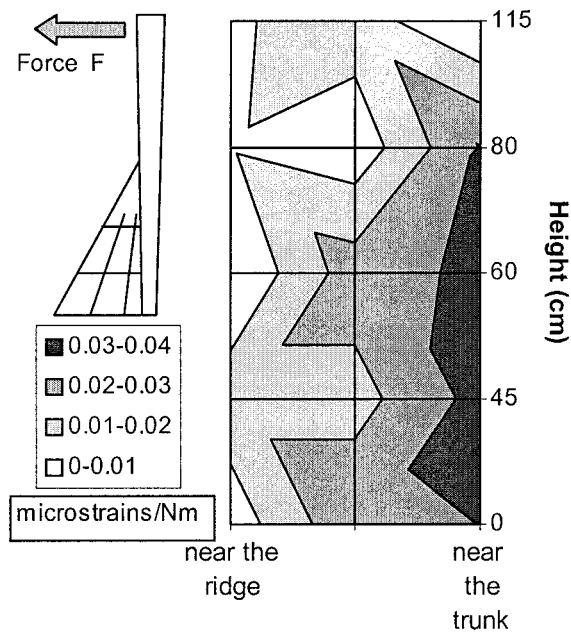
Model and experiment—Experimental patterns of strain variations were compared with the model prediction. Linear correlations between experimental values (ε_L/F) and theoretical ones $\varepsilon_L/E_L F$, computed from the model and independently measured geometrical data, were calculated for different samples (by splitting the whole set of data into different zones) (Table 1). In a general sense, the model and experimental values fit well, with an estimation of the mean modulus of elasticity of 16 400 MPa, with no significant difference between tension and compression. An example of the evolution of both
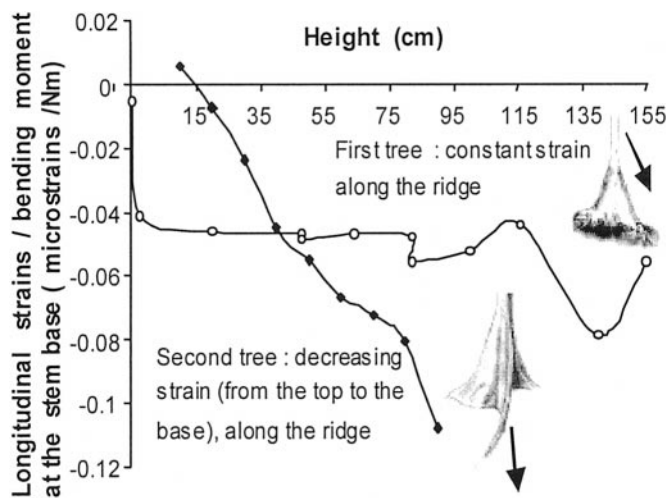

Fig. 6.   Longitudinal strains (ratios to the basal moment) measured during bending tests along the buttress ridges of two *Sloanea* species. In each case, the studied buttress is lined up with the force direction and put in compression. In the first tree, buttresses are plane plates; in the second, buttresses are curved extensions.

Fig. 7.   Breakage observed during bending tests on the second *Sloanea* tree. The cracking buttress is lined up with the force direction and put in compression. Left, just after hearing the first crack; right, after increasing the load.

modeled and experimental strains around the circumference at a given height is given in Fig. 8. However, the correlation coefficient and the modulus of elasticity fit for each cross section increase with height (Table 1). Without great changes of modulus of elasticity from the buttress top to the base, the model does not properly describe developments of strains with height, as indicated by the observed bias on regressions split by ridge or trunk positions. On the same longitudinal line, theoretical strains decrease continuously from the top to the base and measured ones are almost constant.

Wood properties—Measured wood basic density and Young's modulus in buttresses reached the mean value of 0.80 g/cm³ (CV 5%) and 22 160 MPa (CV 35.3%), respectively. The mean Young's modulus predicted from air-dried wood

TABLE 1.   Fitting the experimental strains per unit of applied force (ε_L/F) due to bending tests performed on one buttressed trunk of *Sloanea* cf. *tuerckeimii* to the modeled ratio (beam theory) ε_L/FE_L (E_L: modulus of elasticity). Different correlations have been calculated by splitting data into different zones or sets of tests (column 1). The quality of fit is characterized by r^2 and the observation of bias (asymmetric distribution of residuals). Modulus of elasticity E_L is estimated as the principal axis slope of the graph experiment vs. model.

| Studied part of the tree	Estimated E_L	R^2	Comment
All measured points	16 400 MPa	0.77	No bias
First set of tests (buttress A into traction)	17 400 MPa	0.79	No bias
Second set of tests (buttress A into traction)	15 400 MPa	0.68	No bias
Buttress A only	18 200 MPa	0.77	No bias
Other buttresses only	16 500 MPa	0.68	No bias
Trunk only	14 000 MPa	0.95	Light bias
Ridges only (all buttresses)		0.82	Bias
Sides only (all buttresses)	16 100 MPa	0.69	No bias
100 cm ≤ Height ≤ 140 cm	21 200 MPa	0.90	No bias
80 cm ≤ Height ≤ 120 cm	18 100 MPa	0.84	No bias
60 cm ≤ Height ≤ 100 cm	14 500 MPa	0.83	No bias
40 cm ≤ Height ≤ 80 cm	12 400 MPa	0.75	No bias
20 cm ≤ Height ≤ 60 cm	9900 MPa	0.77	No bias
0 cm ≤ Height ≤ 40 cm	4800 MPa	0.58	No bias
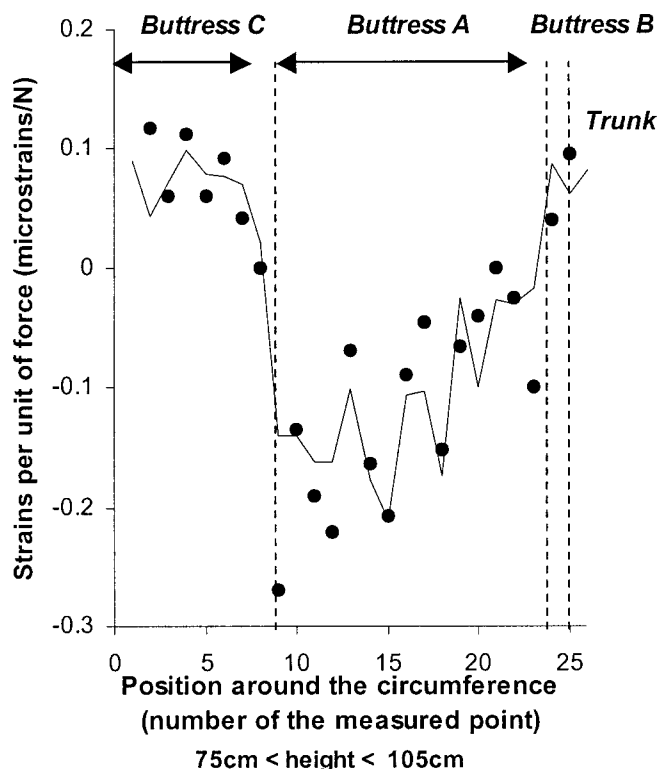
Fig. 8. Variations around the cross section of measured (circles) and modeled (solid line) values of strains due to bending of *Sloanea* cf. *tuerckeimii*. Example of height 90 cm, for buttress A in compression. Abscissa are the order of measured points around the cross section. The modulus of elasticity used in the simulation is the mean value for all the measured points (see Table 1).

density is 22 550 MPa for air-dried wood. Therefore, the Young's modulus of green wood was expected to be 16 180 MPa (value calculated from measured Young's modulus of air-dried wood) or 16 460 MPa (value calculated from density measurements). In two-factor ANOVA, basic density varied significantly with both height and radial position with a strong interaction ($P < 0.001$ for each effect, Fig. 9). Patterns of variations were not regular with respect to height, neither for the mean values nor ridge values. For Young's modulus, variations with depth were not significant. Very high values were measured in upper parts, with no significant variations below 100 cm (Fig. 9).

DISCUSSION

Linearity, elasticity, and small strains—As we applied small strains, the structural behavior remained linear and elastic without any buckling on compressed sides. This is a convenient means of nondestructively measuring strains everywhere by reversible tests and will provide general information about failure risks. However, with this approach, we could not study accurately the modes and localization of failure, except during the breakage experiment on the second tree. Neither could we measure the nonlinear processes that lead to failure.

Modeled and experimental values of longitudinal strains—In a general sense, the model and experimental values fit well. The estimations of the mean green wood Young's modulus (16 400 MPa), when all data were pooled, seemed very realistic, when compared to independent values estimated from tensile tests on air-dried wood specimens or from wood density, although we neglected bark that was very thin compared to stem diameter. The model predicted well the evolution of strains around a circumference (cross section level) and could be used to analyze, for instance, the effect of different force azimuths. However, without great changes of modulus of elasticity from the buttress top to the base, the model did not describe properly the evolution of strains with height. As such variations were not observed from tensile tests or density measurements on wood specimen, these great and regular changes of E_L were not realistic, neither on the whole cross section regardless of the radial position, nor on the ridges that would contribute most to flexural stiffness. The odds are that some hypotheses of the model are not robust enough, especially for low and continuous taper and vertical fibers. Such results emphasize the capacities and limits of beam models that are often used in plant biomechanical theoretical studies (Niklas, 1992)
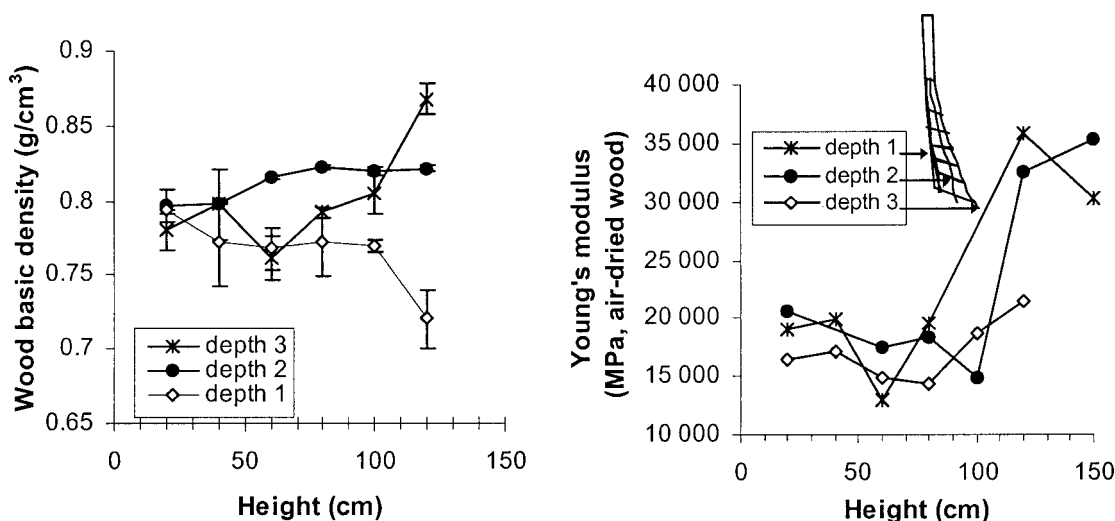

Fig. 9. Variations of wood basic density and Young's modulus measured on wood specimen within buttress A of *Sloanea* cf. *tuerckeimii*. Basic density is the ratio of oven-dried mass vs. green volume. Young's modulus has been measured by tensile tests on air-dried wood.

and scarcely validated by direct assessment of strains and stresses.

Stresses and strains with respect to failure risks—Strains and stresses are three-dimensional. In the principal axes of wood (L, fiber direction; T, tangential direction), at the trunk surface, assuming linear wood behavior, stress components are related to strain components:

$$\sigma_L = E_L(\varepsilon_L + \nu_{TL}\varepsilon_T)/(1 - \nu_{TL}\nu_{LT}) \qquad (a)$$

$$\sigma_T = E_T(\varepsilon_T + \nu_{LT}\varepsilon_L)/(1 - \nu_{TL}\nu_{LT}) \qquad (b)$$

$$\sigma_L = 2G_{LT}\varepsilon_{LT}$$

where E_L and E_T are moduli of elasticity in L and T directions, ν_{LT} and ν_{TL} are Poisson's ratios, and is the G_{LT} shear modulus in LT plane (Guitard, 1987; Niklas, 1992). Because we measured ε_T and ε_L strains of the same order of magnitude, and as $\nu_{TL} \ll 1$ ($\nu_{TL} \approx -0.03$ [Niklas, 1992]), ε_T has no significant effect on σ_L in Eq. a, which then becomes

$$\sigma_L \approx E_L\varepsilon_L(1 - \nu_{TL}\nu_{LT}) \approx E_L\varepsilon_L$$

Thus, Eq. 2 (see Appendix), implicitly assumed by other authors (e.g., Ennos, 1995), is verified and wood follows approximately a simple one-dimension Hooke's law in the longitudinal direction.

However, values of tangential stress σ_T, often neglected, could be of great importance as wood is very weak when submitted to tangential tensile stresses. When tangential stresses are zero, the ratio $\varepsilon_T/\varepsilon_L$ is $-\nu_{LT}$, and $\nu_{LT} \approx 0.67$ (Guitard, 1987; Niklas, 1992). Statistical correlation between ε_T and ε_L was significant, with a ratio $\varepsilon_T/\varepsilon_L$ of -0.64. Thus, mean tangential stresses σ_T are proved to be statistically near zero. They are tensile for points above the regression line $\varepsilon_T/\varepsilon_L = -\nu_{LT}$ and compressive for points below. For example, sides of buttress A are on average put into tangential tension during the first set of tests. Tangential stresses are more likely to be low near the ridge where the relation $\varepsilon_T/\varepsilon_L = -0.64$ is the most significant. They can be high on buttress sides where no relation between $\varepsilon_T/\varepsilon_L$ has been found. For example, in the second tree, by substituting in Eq. b values of the measured ratio $\varepsilon_T/\varepsilon_L$ on the buttress side, we prove that σ_T is safe in compression on the convex side, but dangerous in tension on the concave one. Indeed, this tangential tension, superposed on the high shear, provoked the crack observed during breakage of the tree (Fig. 8).

Mattheck's theory—To analyze our data with respect to the constant stress theory, we need to define stress, because the stress field is defined by three components at the stem surface. Then we must design a stress index, which is calculated from these three components and able to predict locally the risks of failure. The choice of such a failure criterion is still a vexing problem in highly anisotropic materials (Berthelot, 1999): Standards are maximal strain or stress criterions (each strain or stress component is compared to a limit experimentally determined by straight forward uni-axial tests); however, additional interactive criteria able to describe the material behavior under complex triaxial loadings can be designed (Berthelot, 1999). Although Mattheck (Mattheck, 1990; Mattheck and Prinz, 1991) used the interactive Von Mises' criterion, we prefer to use a simple maximal strain or stress criterion that was implicitly used by other authors (Ennos, 1995; Crook et al.,

1997). Indeed, Von Mises' criterion is not adapted to anisotropic materials (Berthelot, 1999). For instance, it predicts the same risk of failure for a tension of 10 MPa in the longitudinal direction than in the tangential one, although it is well known that the former is safe and the latter not. Therefore, in bending experiments in which longitudinal normal stresses σ_L (tension and compression along wood grain) are obviously greater, Von Mises' criterion focuses on these stresses and neglects other components. Actually, along and near the ridges, where σ_L would be the only significant stress, Von Mises' and maximal stress criteria are similar. In this part of the buttress, we found two very different patterns: the first tree follows the constant stress law, but the second one is much more stressed at the buttress top. Both behaviors have been reported (Ennos, 1995; Crook et al., 1997). According to Mattheck's theory, the first tree buttress would have reached its morphologically optimized steady state. The second tree is still optimizing its buttress form. However, such assertions should be demonstrated and, as pointed out by Ennos (1995), Mattheck's theory could not be verified by static data without chronological observations of dynamic growth in natural or experimental conditions. The mechanism of strain perception that controls growth locally is still a puzzling question. Nevertheless, regardless of adaptive theories, the different buttress shapes (plate or shell) of the two trees can explain the different observed patterns of strains, because in the second tree, the buttress base is almost perpendicular to the bending plane.

Moreover, neglecting stress components other than longitudinal ones is not relevant, because breakage modes are obviously not simple compression cracks on the buttress ridges where longitudinal stresses are the highest. In the studied trees, the greatest risks of failure are related to shear and tangential tensions, even though values of these stress components are smaller than the longitudinal ones (wood is less stiff, but also less strong in these strain modes). Although some authors discussed the mechanisms of transverse or shear strengthening in trees (Mattheck, 1991), potential adaptations of tree growth in respect to these strain or stress modes in buttresses have not yet been studied. If, as often supposed, buttresses are material-saving devices, selected for more anchorage stiffness and strength with less volume and less physiological expenditure, in an environment with intense biotic competition for light and space, they have to deal with a mechanical trade-off between minimizing uprooting on one hand and risks of shear and tangential failure in the plates on the other hand. The ecological question is then to estimate the importance of the second constraint: do buttresses fail at the plates? Obviously, the answer will depend on site conditions such as soil types, on buttress shapes, and ontogenetic stages of species.

LITERATURE CITED

BERTHELOT, J. M. 1999. Matériaux composites. Comportement mécanique et analyse des structures. Editions Tec & Doc, Paris, France.

BLACK, H. L., AND K. T. HARPER. 1979. The adaptive value of buttresses to tropical trees: additional hypotheses. *Biotropica* 11: 240.

CHAPMAN, C. A., L. KAUFMAN, AND L. J. CHAPMAN. 1998. Buttress formation and directional stress experienced during critical phases of tree development. *Journal of Tropical Ecology* 14: 341–349.

CLAIR, B., J. RUELLE, AND B. THIBAUT. 2003. Relationship between growth stresses, mechano-physical properties and proportion of fibres with gelatinous layer in chestnut (*Castanea sativa* Mill.). *Holzforschung* 57(2): 189–195.

CROOK, M. J., A. R. ENNOS, AND J. R. BANKS. 1997. The function of buttress roots: a comparative study of the anchorage systems of buttressed (*Aglaia*

and *Nephelium ramboutan* species) and not-buttressed (*Mallotus wrayi*) tropical trees. *Journal of Experimental Botany* 48: 1703–1716.

ENNOS, A. R. 1993. The function and formation of buttresses. *Tree* 8: 350–351.

ENNOS, A. R. 1995. Development of buttresses in rainforest trees: the influence of mechanical stress. *In* M. Coutts and J. Grace [eds.], Wind and trees, 293–301. Cambridge University Press, Cambridge, UK.

FOURNIER, M., B. CHANSON, B. THIBAUT, AND D. GUITARD. 1994. Mesures des déformations résiduelles de croissance à la surface des arbres en relation avec leur morphologie. Observations sur différentes espèces. *Annales des Sciences Forestières* 51: 249–266.

GENTRY, A. H. 1993. A field guide for the families and genera of woody plants of North West South America (Colombia, Ecuador, Peru) with supplementary notes on herbaceous taxa. Conservation International, Washington, D.C., USA.

GUITARD, D. 1987. Mécanique du bois et composites, Cepadues Editions, Toulouse, France.

HALLE, F., R. A. A. OLDEMAN, AND P. B. TOMLINSON. 1978. Tropical trees and forests. An architectural analysis. Springer Verlag, New York, New York, USA.

HOLLOWEL, T., P. BERRY, V. FUNK, AND C. KELLOF. 2001. Preliminary check list of the plants of the Guiana Shield. Smithsonian Institution, Washington, D.C., USA.

KAUFMAN, L. 1988. The role of developmental crises in the formation of buttresses: a unified hypothesis. *Evolutionary Trends in Plants* 2: 39–51.

KOLLMAN, F. F. P., AND W. A. COTE. 1968. Principles of wood science and technology. I. Solid wood. Springer-Verlag, New York, New York, USA.

MABBERLEY, D. J. 1997. The plant book. A portable dictionary of the vascular plants. Cambridge University Press, Cambridge, UK.

MATTHECK, C. 1990. Design and growth rules for biological structures and their application to engineering. *Fatigue and Fracture of Engineering Materials Structures* 13: 535–550.

MATTHECK, C. 1991. Trees: the mechanical design. Springer Verlag, Heidelberg, Germany.

MATTHECK, C., AND M. PRINZ. 1991. Buttress root: why they grow and what they are good for. Internal Report. Karlsruhe Nuclear Research Centre, Karlsruhe, Germany.

NIKLAS, K. J. 1992. Plant biomechanics: an engineering approach to plant form and function. University of Chicago Press, Chicago, Illinois, USA.

RICHARDS, P. W. 1995. The tropical rainforest. Cambridge University Press, Cambridge, UK.

YOUNG, T. P., AND V. PERKOCHA. 1994. Treefalls, crown asymmetry, and buttresses. *Journal of Ecology* 82: 319–324.

APPENDIX

The beam model for longitudinal stress and strain assumes the following hypotheses:

i. The trunk is vertical, i.e., all the centers of mass of each cross section are aligned on a vertical line x. The taper is continuous and low. Wood grain (i.e., longitudinal direction of fibers) is everywhere approximately parallel to the vertical x. Clearly, the two last assumptions are best adhered to with higher cross sections and less developed buttresses. Trunk displacements remain small.

ii. An initial plane cross section remains straight during bending strains. Therefore, at each height x, longitudinal strains $\varepsilon_L(x,y,z)$ within the cross section (y and z are coordinates in a horizontal plane, y in the same vertical plane of the applied force F) are a function of only three unknown parameters: one elongation $\varepsilon_0(x)$ and two curvatures $k_1(x)$ and $k_2(x)$ as

$$\varepsilon_L(x,y,z) = \varepsilon_0(x) + k_1(x)y + k_2(x)z \qquad (1)$$

iii. The stress vs. strain in wood behavior can be simplified into:

$$\sigma_L(x,y,z) = E_L(x,y,z)\varepsilon_L(x,y,z) \qquad (2)$$

Henceforth, the modulus of elasticity E_L will be assumed to be constant within the cross section, but this assumption is easily modified if significant variations of E_L with y or z are observed.

Following this, forces that act on each cross section (height x) during the tests are calculated as

$$N(x) = -F\sin\theta, \qquad M_z(x) = F\cos\theta(L - x), \qquad M_y(x) = 0 \qquad (3)$$

where F is the applied force. L is the distance from the ground to the belt that attaches to the cable and thus, at height x, $(L - x)$ is the lever arm due to bending. θ is the angle between F and the horizontal. N is the normal force (compression due to the vertical component of the force F), M_z and M_y are, respectively, the bending moments around z and y (i.e., the products of the horizontal components of the force F by the lever arm).

Using the strength of materials (Niklas, 1992; Berthelot, 1999), $\varepsilon_0(x)$, $k_1(x)$ and $k_2(x)$ can be calculated from Eqs. 1, 2, and 3 as

$$\varepsilon_0(x) = -F\sin(\theta)/[E_L(x)S(x)]$$

$$k_1(x = F\cos(\theta)(L - x)/\{E_L(x)[I_z(x) - I_{yz}(x)^2/I_y(x)]\}$$

$$k_2(x) = -k_1(x)I_{yz}(x)/I_y \qquad (4)$$

where $S(x)$, I_y, $I_z(x)$, $I_{yz}(x)$ are geometrical characteristics of the cross section: the cross sectional area and the three components of the second moments of area. Hence, $\varepsilon_L(x,y,z)$ can be calculated everywhere from Eqs. 4 and 1.